International Journal of Hydrogen Energy 186 (2025) 152042

Contents lists available at ScienceDirect

International Journal of Hydrogen Energy

journal homepage: www.elsevier.com/locate/he

Dark fermentative biohydrogen production: Bibliometric trends, techno-economic insights, emerging challenges, and sustainable pathways

Moustafa Gamal Snousy [a,**], Ashraf R. Abouelmagd [b], Dimitrios E. Alexakis [c], Hassan Mohamed Helmy [d], Yasser M. Moustafa [e,f], Abdelazim Negm [g], Erik Weiss [h], Roland Weiss [h], Esam Ismail [d,i], Sayed Mohamed Sakr [i,j], Abeer El Shahawy [k], Ahmed M. Saqr [l,m,*]

[a] Egyptian Petroleum Sector, Petrotrade Co., Block 10 - Plot No. 3 - District 11, Nasr City, Cairo, Egypt
[b] Egyptian Petroleum Sector, Egyptian Natural Gas Holding Company, 85 Nasr Road, 1st District, Nasr City, Cairo, Egypt
[c] Laboratory of Geoenvironmental Science and Environmental Quality Assurance, Department of Civil Engineering, School of Engineering, University of West Attica, 250 Thivon & P. Ralli Str., Athens, GR 12241, Greece
[d] Geology Department, Faculty of Science, Minia University, P.O. Box 61519, El-Minia, Egypt
[e] Analysis and Evaluation Department, Egyptian Petroleum Research Institute (EPRI), 1 Ahmed El Zomor St., Nasr City, 11727, Cairo, Egypt
[f] Central Analytical Laboratories, Nanotechnology Research, Egyptian Petroleum Research Institute (EPRI), 1 Ahmed El Zomor St., Nasr City, 11727, Cairo, Egypt
[g] Department of Water and Water Engineering, Faculty of Engineering, Zagazig University, Zagazig, Egypt
[h] University of Economics in Bratislava, Faculty of Business Economy with Seat in Košice, Slovakia
[i] Geology Department, College of Science, Taibah University, Medina 344, Saudi Arabia
[j] Geology Department, Faculty of Science, Al-Azhar University, Cairo, Egypt
[k] Department of Civil Engineering, Faculty of Engineering, Suez Canal University, P.O. Box 41522, Ismailia, Egypt
[l] Irrigation and Hydraulics Department, Faculty of Engineering, Mansoura University, Mansoura, 35516, Egypt
[m] Cologne University of Applied Sciences (TH Köln), Cologne, Germany

ARTICLE INFO

Handling Editor: Suleyman I. Allakhverdiev

Keywords:
Ultra-green hydrogen
Dark fermentation
Circular economy
Techno-economic analysis
Bibliometric analysis
Sustainable development goals

ABSTRACT

Global energy demand has risen sharply, intensifying concerns over greenhouse gas emissions and climate change. Fossil fuel combustion remains the primary driver of increasing carbon dioxide levels. A rapid transition to clean energy sources is therefore imperative. Dark fermentative biohydrogen production (DFHP) has been investigated as a scalable, low-carbon hydrogen (H_2) pathway that leverages organic waste and industrial waste heat. The study objectives were to quantify research evolution, assess techno-economic performance, and propose sustainable deployment pathways. Bibliometric analysis was performed on 435 Scopus records, yielding an annual growth rate of 19.6 % and 928 unique keywords. Besides, bibliometric trends were visualised using VOSviewer, Biblioshiny, and Graphica software. For techno-economic evaluation, H_2 conversion efficiencies, water requirements, and cost impacts under waste-heat integration were compared against conventional H_2 production methods. DFHP was shown to operate in standard fermenters with negligible water demand. Waste-heat integration was demonstrated to eliminate external heating costs and lower levelized H_2 costs. Key technical and operational challenges were identified, including feedstock variability, volatile metabolite inhibition, and mass- and heat-transfer limitations at scale. Sustainable pathways were outlined, emphasizing low-energy pretreatment, in situ metabolite removal, advanced reactor geometries, and inclusive capacity-building partnerships co-located with waste-processing facilities. Alignment with sustainable development goals (SDGs) for affordable clean energy, responsible consumption, and climate action was highlighted. A clear roadmap has been provided to advance global decarbonization efforts and to accelerate the deployment of a resilient H_2 economy.

* Corresponding author.
** Corresponding author.
E-mail addresses: moustafa_gamal93@yahoo.com (M.G. Snousy), Dr.ashraf.abouzaid@gmail.com (A.R. Abouelmagd), d.alexakis@uniwa.gr (D.E. Alexakis), hmhelmy@yahoo.com (H.M. Helmy), ymoustafa12@yahoo.com (Y.M. Moustafa), amnegm@zu.edu.eg (A. Negm), erik.weiss@euba.sk (E. Weiss), roland.weiss@euba.sk (R. Weiss), essam.ismail@mu.edu.eg (E. Ismail), smsakr@taibahu.edu.sa (S.M. Sakr), abeer_shahawi@eng.suez.edu.eg (A. El Shahawy), ahmedsaqr@mans.edu.eg, ahmed.saqr@th-kolen.de (A.M. Saqr).

https://doi.org/10.1016/j.ijhydene.2025.152042
Received 11 August 2025; Received in revised form 27 September 2025; Accepted 14 October 2025

1. Introduction

Global energy consumption jumped from 104,722 tera watt-hours (TWh) in 2000 to 168,233 TWh in 2019 and is expected to rise by 80 % to roughly 302,819 TWh by 2050, driven by population growth and economic expansion [1,2]. Over half of this demand is met by burning fossil fuels, e.g., oil, coal, and natural gas, pushing primary energy use from 13,647 million tonnes of oil equivalent (Mtoe) in 2015 to 14,477 Mtoe in 2021 [3,4]. This carbon-intensive mix accounts for 84 % of global energy and underpins a 6 % rise in energy- and industry-related carbon dioxide (CO_2) emissions, which reached 36.3 billion tonnes in 2021 [5]. Meanwhile, atmospheric greenhouse gas concentrations peaked in 2018 at 407.8 parts per million (ppm) CO_2, 1869 parts per billion (ppb) Methane (CH_4), and 331 ppb Nitrous Oxide (N_2O), fueling global warming and heightening climate risk [6,7]. To align with Intergovernmental Panel on Climate Change (IPCC) and International Energy Agency (IEA) targets, CO_2 must fall 45 % by 2030 on the route to net-zero by 2050, making a rapid shift to affordable, reliable clean energy [8,9]. Snousy et al. [10] highlight biomass-driven hydrogen (H_2) via dark fermentation, augmented by waste-heat integration, as a means to access low-cost H_2 in Africa, illustrating the dual benefits of renewable feedstocks and process intensification.

H_2's appeal lies in its high energy density (~122 kJ g^{-1}) and zero-emission end-use, powering electricity generation, ammonia synthesis, and fuel upgrading without CO_2 by-products [11]. Concepts of a "hydrogen economy" and "hydrogen cities" date back to the 1970s and 1980s [12]. However, Europe's recent gas crisis and market volatility following the Russia–Ukraine conflict have revitalised strategic H_2 investments [13,14]. In 2019, the global H_2 market exceeded USD 140 billion and is forecast to grow at a compound annual growth rate (CAGR) of over 6.25 % through 2026 [15], while the International Renewable Energy Agency (IRENA) projects that annual H_2 demand must reach 614 Mt to meet net-zero pathways [16]. Yet 95 % of today's 120 Mt y^{-1} production stems from fossil feedstocks, predominantly grey H_2, with blue H_2 still energy-intensive, leaving bio-based-H_2 uncompetitive absent large subsidies and capital influx [7,17]. High capital expenditure (CAPEX) for electrolysers and water requirements further constrain renewable-based H_2, especially in developing regions where external financing is scarce [18].

Addressing these challenges requires innovative, low-carbon pathways [19]. Dark fermentative biohydrogen production (DFHP) converts organic substrates, e.g., agricultural residues, wastewater sludge, and food waste, into H_2 under anaerobic, light-independent conditions, achieving high conversion efficiencies across mesophilic to hyperthermophilic regimes [20]. Unlike electrolysis, DFHP operates in standard fermenters, demands minimal water, and exploits waste-heat integration to eliminate external heating costs. Pre-treatment methods (e.g., mild alkaline hydrolysis) improve feedstock uniformity, while in situ removal of volatile fatty acids mitigates microbial inhibition [21]. Advanced reactor designs, i.e., multi-stage packed beds and continuous-flow loops, enhance mixing and heat transfer, addressing scale-up constraints [22]. However, feedstock variability, metabolite inhibition, and pilot-scale validation remain hurdles [23]. Overcoming these will unlock DFHP's potential as a scalable, low-carbon H_2 platform, complementing electrolytic routes and advancing global decarbonization efforts [24].

This review critically examines bibliometric trends and techno-economic insights in DFHP from 2006 to 2025. Six key dimensions were mapped: H_2 colour spectrum and principal production technologies; emerging clean H_2 pathways; bioreactor modelling; electrolysis versus dark fermentation comparisons; dual waste-reduction and energy-recovery roles of bio-based H_2; and cost dynamics with waste-heat integration. Then, technical and operational challenges, such as feedstock variability, microbial inhibition, and scale-up constraints, were identified, and sustainable pathways aligned with the Sustainable Development Goals (SDGs) were identified. Novelty lies in integrating bibliometric analysis with detailed techno-economic evaluation to chart a cohesive framework for scaling DFHP. Study objectives are: (a) to quantify research evolution and collaboration networks via bibliometric methods; (b) to critically compare process economics and efficiencies across H_2 production routes; and (c) to recommend targeted technological and policy interventions to unlock DFHP's potential as a scalable, low-carbon H_2 platform. This integrated perspective aims to inform future research, guide policy development, and accelerate DFHP deployment, thereby making a tangible impact on decarbonising global H_2 supply chains.

2. Research methodology

The research followed a sequential methodological workflow as outlined in Fig. 1.

2.1. Data collection

This study systematically retrieved publications on DFHP from the Scopus database, selected for its comprehensive coverage of energy and environmental research and consistent metadata standards [25]. The search string "Biohydrogen" AND "dark" AND "fermentation" AND "sustainab*" was applied to titles, abstracts, and author keywords for documents published between January 2006 and August 2025. Filters limited results to English-language articles, review articles, book chapters, and conference papers, reflecting that over 99 % of retrieved records were in English. Records lacking essential metadata, those outside the defined date range or document types, and duplicate entries identified via matching DOIs were removed. The remaining publications were exported in CSV format, capturing author names, affiliations, publication details, abstracts, keywords, citation counts, and references. This rigorously curated dataset underpins the subsequent bibliometric

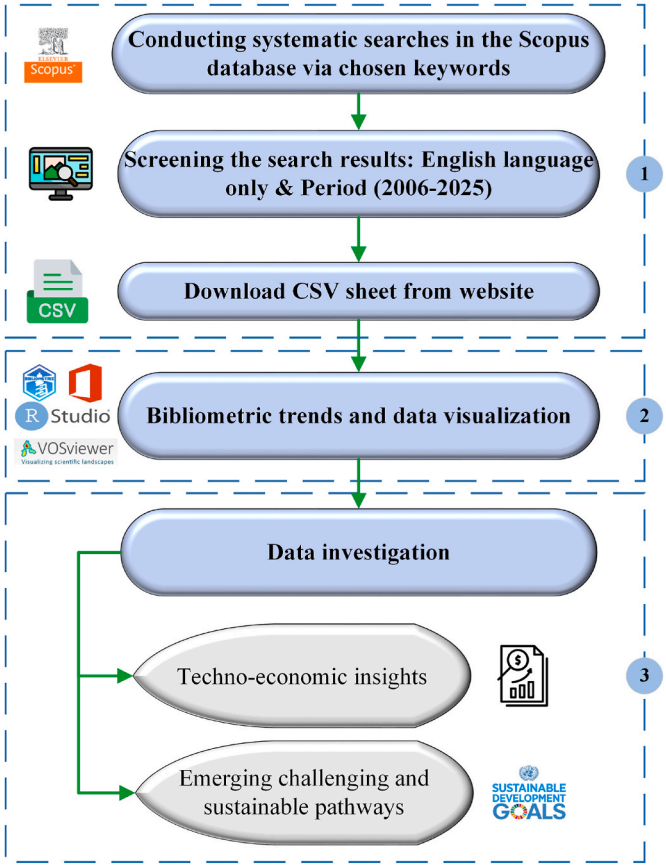

Fig. 1. A schematic diagram of the research methodology.

and thematic analyses.

2.2. Data visualization

Bibliometric analyses were performed using Biblioshiny (Bibliometrix R package), VOSviewer (version 1.6.18), Scimago Graphica, and Microsoft Office tools. First, Biblioshiny generated descriptive metrics, including the annual publication growth rate, number of distinct authors, keyword diversity, average citations per document, and co-authorship patterns among researchers. These metrics provided a quantitative overview of research output trends and collaboration intensity [26]. Second, VOSviewer was applied to visualise thematic structures through keyword co-occurrence mapping [27]. Author keywords were imported to construct a network wherein node size reflects term frequency and link strength indicates co-occurrence intensity. Clustering algorithms identified major research themes and their interrelations. Third, Scimago Graphica was used to create radial graphs that visualise author collaboration patterns. Its visualization tools made it possible to clearly depict relationships and connections within the research network [28]. Finally, Microsoft PowerPoint and Visio were used to produce precise, publication-quality bibliometric figures [29]. PowerPoint enabled rapid assembly of engaging flowcharts, organisational diagrams, and animations. Visio delivered detailed flow diagrams, network maps, and process schematics with exact control over connectors and data. Integrating Visio diagrams into PowerPoint combined technical accuracy and presentation versatility [30].

2.3. Data investigation

A multi-dimensional appraisal was conducted to evaluate six key aspects of DFHP research through a techno-economic lens.

- H_2 colour spectrum and main production technologies: Studies were categorized by H_2 "color" classification and primary production routes (e.g., steam methane reforming, coal gasification, electrolysis, dark fermentation), with associated CO_2 emission factors.
- Main clean H_2 production directions: H_2 pathways, including electrolytic, photobiological, and thermochemical processes, were mapped according to feedstock type, process maturity, and energy inputs.
- Structure, temperature, and heat-transfer processes of bioreactor modelling: Reactor design parameters, dynamic heat-balance equations, and operational temperature setpoints were extracted to compare modelling approaches for jacketed, stirred–tank fermenters.
- Technical and economic comparison of DFHP vs. electrolysis versus: Levelized cost of energy (LCOE) and H_2 (LCOH) metrics were compiled under equivalent CAPEX/Operating Expenditure (OPEX) assumptions to benchmark electrolytic against dark fermentation systems with waste-heat integration.
- Dual role in waste reduction and energy production in bio-based H_2: Techno-economic data on substrate conversion efficiencies and by-product valorization were analysed to quantify waste minimization benefits alongside H_2 yields.
- Cost evolution of incorporating bio-based hydrogen production and waste-energy recovery: Historical LCOH trends were traced to assess how harnessing free thermal inputs shifts cost structures over the project lifetime.

For each dimension, relevant cost and performance parameters were standardized in a comparative template. Sensitivity analyses tested the impact of key variables (e.g., energy transformation efficiency, feedstock heterogeneity) on economic outcomes. These methods established a rigorous foundation for identifying emerging challenges and framing sustainable pathways for DFHP research.

3. Results and discussion

3.1. Bibliometric trends

3.1.1. Statistics associated with publications

The bibliometric analysis revealed that DFHP research had undergone robust expansion between 2006 and 2025 (Fig. 2). Over these 20 years, 1682 distinct authors contributed to 435 peer-reviewed documents, published across 189 different outlets, demonstrating both depth and diversity in the field. Authors used 928 unique keywords, underscoring the proliferation of specialized topics, from reactor configuration to metabolic engineering, within this research community. Publication output increased at a compound annual growth rate of 19.6 %, reflecting accelerating interest and resource allocation toward microbial H_2 strategies. Collaborative patterns were notable: the average number of co-authors per document was 5.13, and nearly 38 % of papers involved international partnerships, highlighting the global coordination essential for advancing process optimization and scale-up studies. Impact metrics further emphasise the field's maturity. Each document accrued an average of 36.64 citations, indicating that key methodological developments, such as techno-economic frameworks for reactor integration, have become foundational references for subsequent investigations. The document's average age of 4.39 years suggested that the community continually built upon recent findings rather than relying solely on older paradigms. Taken together, these statistics paint a picture of a dynamic, high-impact research arena characterized by rapid growth, thematic diversification, and strong international collaboration [31]. This bibliometric profile aligns with broader trends in bioenergy research, where interdisciplinary teams leverage shared data and standardized methods to accelerate progress toward scalable, low-carbon H_2 solutions [32].

3.1.2. Collaboration patterns

The author collaboration network revealed two dominant groups (Fig. 3a). One group was anchored by researchers such as Gupta, Haque, Mishra, and Srivastava, characterized by dense interconnections that indicate multiple co-authored studies. The second group focused on other authors, such as Chang, Lee, and Bhatti, suggesting the expansion of regional involvement. The country collaboration map (Fig. 3b) highlighted India's central role, shown by the darkest shading and numerous outbound links. Strong bilateral ties connected India to China, the United States, and Australia. China further established extensive links with the United Kingdom and Germany. Europe–North America connections were present but less pronounced than those between Asia and the West, reflecting strategic partnerships that leverage varied regulatory environments and feedstock availability. These patterns mirror trends observed in bioenergy research, where geographically diverse consortia accelerate technology validation through the use of shared pilot facilities and standardised protocols [33]. Such international networks have been demonstrated to enhance replicability and reduce the time to scale up in fermentation-based processes [34].

3.1.3. Keyword Co-occurrence

The keyword co-occurrence network (Fig. 4) revealed four tightly knit thematic clusters in DFHP research. The red cluster is centered on core fermentation processes. It included "dark fermentation," "biohydrogen production," "fermentation," "biohydrogen," and "hydrogen production," with strong links to "anaerobic digestion," "substrates," "renewable energy," "wastewater treatment," and "volatile fatty acids," indicating sustained focus on microbial pathways and diverse waste feedstocks. The yellow cluster highlighted feedstock processing. Its nodes, e.g., "biomass," "lignocellulosic biomass," "H_2 production," "pretreatments," and "pre-treatment," were closely connected, reflecting frequent coupling of pre-treatment methods with yield optimization studies. The green cluster represented integration into broader biofuel systems. It comprised "hydrogen," "biofuel," "biofuels," "metabolism,"

Fig. 2. Highlights from publication trends dark fermentative biohydrogen (DFHP) research (2006–2025).

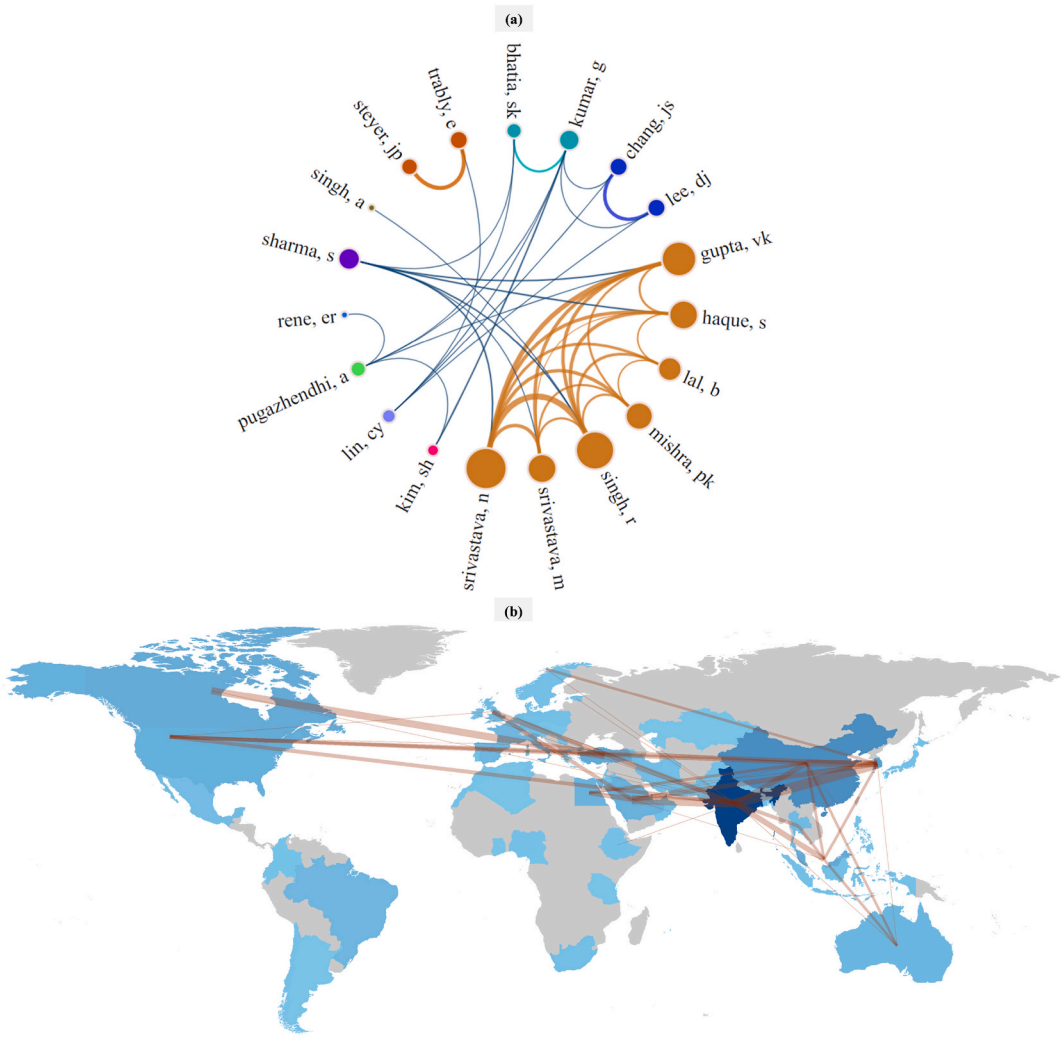

Fig. 3. Collaborative pattern associated with dark fermentative biohydrogen (DFHP) research (2006–2025): (a) author, and (b) country collaboration network.

"bioreactor," "article," "sustainability," and "bioenergy," underscoring research that situated dark fermentation within renewable energy portfolios. The blue cluster addressed alternative production routes and sustainability framing. It joined "sustainable development," "fossil fuels," "microorganisms," "photobiological hydrogen production," "photolysis," "microalgae," "electrolysis," and "greenhouse gases," pointing to comparative analyses of dark versus light-driven processes and life-cycle considerations. Edge thickness highlighted that the strongest co-occurrences occur between "dark fermentation" and "bio-hydrogen production," as well as "biohydrogen" with "hydrogen

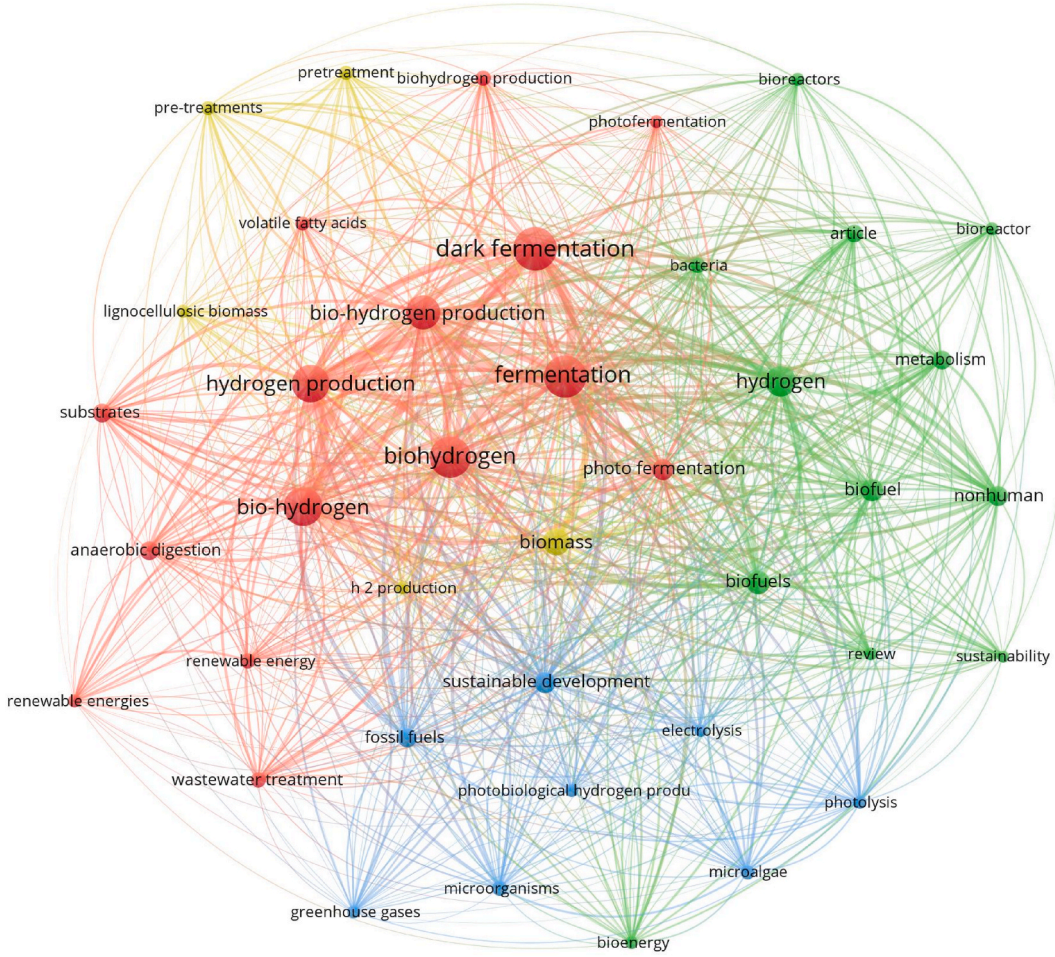

Fig. 4. A network of keyword co-occurrence associated with dark fermentative biohydrogen (DFHP) research (2006–2025).

production," underscoring their central pairing in the literature. These co-occurrence patterns align with earlier reviews that document the shift of the field from foundational kinetics toward integrated studies combining pre-treatment, process modelling, and sustainability assessments [35].

3.2. Techno-economic overview

3.2.1. Hydrogen colour spectrum and main production technologies

H_2 is a colourless, odourless gas that the energy industry classifies into different colour codes, e.g., grey, brown, black, blue, cyan, turquoise, yellow, green, ultra-green, purple, pink, red, and white, to indicate the production method or source. However, these designations lack a universal naming convention and can vary across regions and over time [36,37]. The colour of the H_2 spectrum highlights the divergence between fossil-based and low-carbon production routes. Fossil-derived H_2 remains dominant, with grey, brown/black, and blue H_2, comprising 98 % of the global supply. Grey H_2 via steam methane reforming accounts for 75 % of output and emits 4–12 kg CO_2 per kg H_2 [7]. Brown/black H_2 from coal gasification contributes 23 % and yields 19 kg CO_2 per kg H_2. Blue H_2 adds CCS to reforming or gasification, reducing emissions below 4 kg CO_2 per kg H_2 [38]. Renewable-derived variants occupy a minor share. Green H_2, generated by electrolyzing water with renewable electricity, achieves near-zero emissions and aligns with net-zero targets. Although its market share is currently small, falling electrolyser costs and the expansion of renewable energy sources are accelerating uptake. Ultra-green H_2, produced biologically from biomass via processes like dark fermentation under anaerobic conditions, achieves carbon-negative emissions and supports long-term climate goals [39]. Yellow H_2 (grid-powered electrolysis) carries a high carbon intensity of 29 kg CO_2 per kg H_2 when electricity is fossil-sourced [40], underscoring the need for renewable pairing. Cyan and turquoise H_2 (<1 kg or ~ 0 kg CO_2 per kg H_2) and purple/pink/red H_2 (0–1 kg CO_2 per kg H_2) further illustrate intermediate low-carbon pathways. Globally, 70 Mt of H_2 produced from fossil routes emits 830 Mt CO_2 annually [41]. Transitioning to green and bio-based H_2 could eliminate these emissions, marking a pivotal shift toward sustainable energy systems [42]. These findings illustrate that, alongside declining electrolyzer costs and supportive policies, green H_2 is poised to disrupt the current dominance of fossil-based H_2, with bio H_2 offering additional niche applications in waste valorization and off-grid energy systems [43].

3.2.2. Main clean hydrogen production directions

The four significant H_2 production techniques are: biological, electrical, photonic, and thermal. Each encompasses multiple specialized sub-methods, with several mature technologies already in commercial use and others under development. Biological approaches, in particular, offer routes to enhance efficiency and lower costs by valorizing waste streams and recovering energy from biomass. Biomass serves as a renewable, low-carbon feedstock capable of yielding cumulative low, zero, or even negative greenhouse-gas emissions when integrated into circular conversion processes [44].

DF represents the most mature biological method and constitutes the core of DFHP. DFHP is a biological process that utilizes anaerobic microbial metabolism to convert organic substrates into hydrogen gas without light requirements [45]. This process operates through

facultative and obligate bacteria, predominantly Clostridium species, that possess hydrogenase enzymes capable of catalyzing hydrogen evolution from organic compounds. Under strict anaerobic conditions, diverse bacteria convert carbohydrates into molecular H_2 and soluble by-products. The fundamental importance of DFHP lies in its ability to simultaneously address waste management and clean energy production. It can operate continuously at moderate temperatures (30–60 °C), tolerate diverse feedstock compositions, and achieve rapid hydrogen generation without external energy input for illumination.

Key biochemical pathways include acetate formation (Equation (1)) and butyrate formation (Equation (2)), which yield H_2 through different metabolic routes. The acetate pathway produces 4 mol of hydrogen per mole of glucose, representing the theoretical maximum yield. The butyrate pathway generates 2 mol of hydrogen per mole of glucose but is more energetically favorable for bacterial growth. Solventogenic routes (Equations (3) and (4)) channel electrons into ethanol and lactate instead of H_2, reducing overall hydrogen yields. Additionally, rerouting lactate into butyrate synthesis (Equation (5)) partially restores H_2 potential by redirecting metabolic flux toward hydrogen-producing pathways. Sequential coupling of DF effluent with light-dependent photofermentation further boosts overall H_2 output. In this scheme, photosynthetic bacteria convert residual organic acids into additional H_2 and H_2O under illumination. This integration maximises substrate utilization and streamlines waste management, providing a practical, low-carbon platform for sustainable H_2 generation from biomass [46].

$$C_6H_{12}O_6 + 4H_2O \rightarrow 2CH_3COO^- + 2HCO_3^- + 4H^+ + 4H_2 \quad (1)$$

$$C_6H_{12}O_6 + 2H_2O \rightarrow 2CH_3CH_2CH_2COO^- + 2HCO_3^- + 3H^+ + 2H_2 \quad (2)$$

$$C_6H_{12}O_6 + 2H_2O \rightarrow 2CH_3CH_2OH + 2HCO_3^- + 2H^+ \quad (3)$$

$$C_6H_{12}O_6 \rightarrow 2CH_3CHOHCOO^- + 2H^+ \quad (4)$$

$$CH_3CHOHCOO^- + 0.4CH_3COO^- + 0.7H^+ \rightarrow 0.7\ CH_3CH_2CH_2COO^- + 0.6H_2O + CO_2 + 0.4H_2O \quad (5)$$

3.2.3. *Bioreactor modeling: structure, temperature, and heat-transfer processes*

Bioreactors designed for dark fermentation integrate three core components, i. e, a reaction vessel, an internal stirrer, and an external jacket, to orchestrate simultaneous biochemical conversions under tightly controlled conditions (Fig. 5a). Feedstock enters the vessel, where facultative and obligate anaerobes metabolize carbohydrates in a liquid medium, generating H_2 and various organic byproducts. The stirrer facilitates uniform suspension of cells, enhances gas–liquid dispersion, and minimizes substrate and temperature gradients [47]. Meanwhile, the jacket encloses the vessel to isolate it thermally from ambient fluctuations. Circulating a cooling fluid through the jacket extracts metabolic heat, sustaining a stable setpoint temperature essential for optimal hydrogenase activity [48]. The effectiveness of this thermal regulation is evidenced by consistent temperature profiles that align with maximal H_2 production rates. Temperature shifts from the optimal 55 °C–35 °C cause significant yield reductions of 27 % in dark fermentation systems [49]. Optimal hydrogen production occurs at controlled temperatures of 33 °C with maximum hydrogenase activity in temperature-varying systems [50]. Thermal excursions beyond these ranges denature microbial enzymes and impair yields significantly. The jacket-mediated heat dissipation prevents such thermal excursions by maintaining stable reactor temperatures. This thermal control is critical for preserving enzyme functionality and maximizing biohydrogen yields [51].

Temperature control emerges as a decisive parameter for process scalability and productivity [52]. Anaerobic H_2 fermentation proceeds exothermically; microbial growth and metabolism continually produce heat, rendering temperature homogeneity challenging, especially in larger volumes where mixing limitations foster hot spots [53]. Empirical observations reveal a distinct hysteresis loop in temperature response during heating and cooling cycles (Fig. 5b). During the heating phase, the reactor temperature swiftly climbs due to combined metabolic and external heating inputs; during cooling, the decline is more gradual, reflecting thermal inertia and convective mixing delays. The resulting loop underscores asymmetric heat-transfer characteristics that narrow

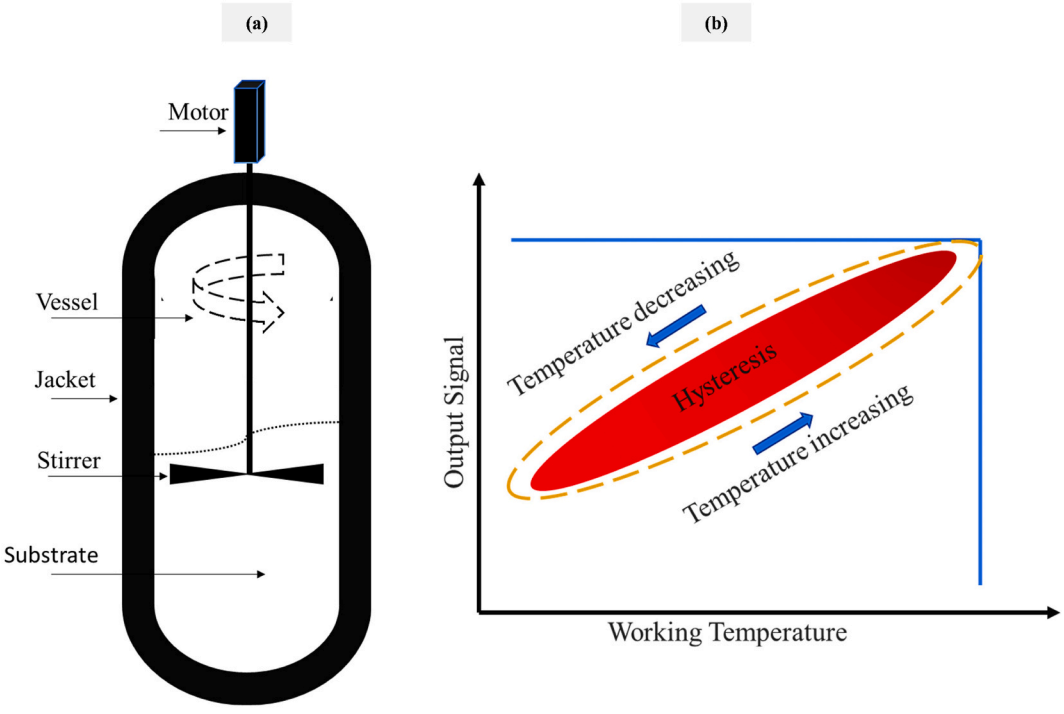

Fig. 5. Bioreactor details designed for dark fermentation: (a) schematic illustration of its structure, and (b) its temperature hysteresis. Original illustration by authors based on literature synthesis of dark fermentation bioreactor design principles.

the window of optimal operation [54]. Enhancing heat-transfer area and stirrer power input significantly reduces the hysteresis loop's area, thereby extending the duration of the constant-temperature plateau where H_2 production is maximized [55]. Mathematical models incorporating time-delay parameters and transient heat-transfer coefficients demonstrate close alignment with these observations, underscoring the importance of precise integration of structural design and dynamic thermal control in maintaining microbial viability and sustaining high H_2 production across scales [56].

Despite their widespread use, the nuances of heat transfer in stirred bioreactors remain only partially understood. As reactor intensification and novel microbial strains expand operational capabilities, effective thermal management becomes ever more critical. Real-world fermentation involves multiple, overlapping heat flows (metabolic, mechanical, and jacket exchange), making overall heat transfer difficult to quantify [57]. To address this, various conservation models have been proposed. For instance, Hu et al. [47] presented a unified temperature-control framework spanning 0–100 °C, mathematically describing reactor dynamics via Equation (6) and jacket behaviour via Equation (7).

$$\frac{d}{dt}\begin{bmatrix} T \\ T_j \end{bmatrix} = \begin{bmatrix} -a_1\,(T - T_j) \\ a_2\,(T - T_j) + a_3\,(T_0 - T_j) \end{bmatrix} + \begin{bmatrix} 0 \\ 1 \end{bmatrix} U \tag{6}$$

$$Y = T \tag{7}$$

where the tank-side temperature is T; T_j is the temperature of the jacket (sheath); T_0 is the ambient (room) temperature; Y is the output; U is the input; a_1, a_2, and a_3 are the thermal conductivity coefficients of the tank from inside to outside, respectively. As a_1 and a_2 are the thermal conductivity coefficients of the reactant in the tank from inside to outside, $a_1 = a_2$; and under the condition of neglecting the loss of thermal ($a_3 = 0$), T(s) can be defined as in Equation (8).

$$T(S) = \frac{a_1 U(S)}{S^2 + 2a_1 S} = \frac{K_m}{S(T_m S + 1)}\,U(S) \tag{8}$$

where S is an *S*-function or system functions that define the method of a block works through diverse simulation parts, for example, initialization, update, derivatives, outputs, and termination, K_m is a coefficient, and $T_m = 1/2a_1$. Considering the time delay (L_m), the temperature model, described in Equation (9), integrates the process with the time delay.

$$T(S) = \frac{K_m e^{-L_m}}{S(T_m S + 1)}\,U(S) \tag{9}$$

Despite model disturbances and uncertainties, Tusset et al. [58] showed a mathematical model of desired temperature levels in bioreactors. The proposed mathematical model was developed to characterise the dynamic behaviour of a bioreactor in which a fermentation process takes place. The reactor temperature is determined by Equation (10), while the temperature variation within the jacket is defined by Equation (11).

$$\frac{d(T_r)}{dt} = \frac{F_i}{V}(T_{in} + 273) - \frac{F_e}{V}\,(T_r + 273) + \frac{rO_2 \Delta H_r}{32_{\rho r} C_{heat,r}} - \frac{K_T A_T (T_r - T_{ag})}{V_{\rho r} C_{heat,r}} \tag{10}$$

$$\frac{d(T_{ag})}{dt} = \frac{F_{ag}}{V_j}\,(T_{in,ag} - T_{ag}) + \frac{K_T A_T (T_r - T_{ag})}{V_{j\rho ag} C_{heat,ag}} \tag{11}$$

where T_r are the inside reactor temperatures, T_{ag} are the temperatures in the jacket, T_{in} are the temperatures in the reactor inlet, F_i is the fermentation vessel inlet flow, F_e is the fermenter outlet flow, F_{ag} is the coolant flow is the jacket, V is the reactor volume, V_j is the jacket volume, rO_2 rate of oxygen variation (the equilibrium oxygen level within the fermenter is heat dependent), ΔH_r is the heat flows difference of the reactor, K_T is a maximum temperatures progress rate, A_T is the temperature state matrix, ρ is the average density of the reactants that exist inside the reactor, C are the capacities.

Tang et al. [54] displayed a mathematical model to control reactor temperature for improving fractional order self-*anti*-disturbance, assuming that the material is well blended, the volume is unchanged, the heat capacity is unchanged, etc., the dynamic equilibrium equation of heat in the reaction is applied by Equation (12).

$$\frac{dT}{dt} = \frac{UA}{v\rho c_p}(T_C - T) + \frac{(\Delta H) C_A}{\rho C_p}\,K_0 e^{-\frac{E}{RT}} \tag{12}$$

where $K = K_0 e^{-\frac{E}{RT}}$, T is the temperature inside the reactor at which the reaction occurs, A is the area of heat transfer in the reactor's jacket, U is the overall heat transfer coefficient of the reactor's jacket, T_C is the temperature at which the jacket is cooling, ΔH is the heat generated by the reaction, C_p is the heat capacity (the average specific heat of the concentration of the reactants inside the reactor), v is the volume of the reactants inside the reactor, ρ is the average density of the contained reactants, C_A is the average concentration of the reactants. K denotes the reaction rate inside a reactor, k_0 signifies the reaction frequency factor at which internal reactants are reacting, E signifies the activation energy, and R characterizes the gas constant.

For the reactor's jacket, the dynamic conservation of heat can be described by the organized Equation (13).

$$\frac{dT_c}{dt} = \frac{F_c}{V_c}(T_j - T_C) + \frac{UA}{V_c \rho_c C_{pc}}(T_j - T_C) \tag{13}$$

where V_c represents the value of the jacketed media volume and reflects its density. C_{pc} stands for the average specific heat of the jacketed media. F_c is the flow rate of jacketed media, T_j is the temperature at which jacketed media are acceptable to enter.

Müller et al. [51] developed a mathematical model of the reactor, provided equations for the stirred reactor presented in Equation (14), and the jacket side obtained in Equation (15).

$$\sum_{t=1}^{n}(m_i \bullet C_{p,i}) \bullet \frac{d\dot{T}_r}{dt} = -U_{rj} \bullet A_{rj} \bullet \Delta T_{log.rj} + q_p + q_s - (UA)_{r,loss} \bullet \Delta T_{ar} \tag{14}$$

$$\sum_{t=1}^{n}(m_i \bullet C_{p,i}) \bullet \frac{d\dot{T}_j}{dt} = U_{rj} \bullet A_{rj} \bullet \Delta T_{log,rj} - F_j \bullet \rho_j \bullet (T_{j,out} - T_{j,in}) - (UA)_{r,loss} \bullet \Delta T_{aj} \tag{15}$$

where U_{rj} is the product of the entire heat transfer coefficient, A_{rj} is the heat transfer area, and ΔT_{log} is the mean logarithmic temperature variance, q is the heat flow, ρ is the density, q_p is the heat source, q_s is the power input by the stirrer, and U_{loss} is the heat loss to the surrounding environment from the exposed surface.

The totality of the heat capacities represents the accumulation term, depicting the progression of heat within the reactor as the temperature rises during the initial warming phase, remains steady in the constant temperature phase, and then decreases through the cooling phase. As m is the substrate mass, and C_p is the specific heat capacity of entirely temperature-varying portions given to this balance space, accordingly, dT_i/dt is the time derivative of the temperature. Assuming all compartments in the balance space are in equilibrium using a standard temperature, $\dot{T}_r$ (Equation (16)) or $\dot{T}_j$ (Equation (17)), respectively. However, Equation (18) calculates heat transfer between the reactor and the jacket [51].

$$\dot{T}_r = T_r \tag{16}$$

$$\dot{T}_j = \frac{T_{j,out} - T_{j,in}}{\ln\left(\frac{T_{j,out}}{T_{j,in}}\right)} \tag{17}$$

$$\Delta T_{log.rj} = \frac{(T_{j,out} - T_{j,in})}{\ln\left(\frac{T_r - T_{j,in}}{T_r - T_{j,out}}\right)} \quad (18)$$

Heat loss to the environment, $U_{loss,}$ is calculated from the exposed surface, assuming the heat transfer coefficient for free convection in gases on a flat plate, and times the driving force (Equations (19) and (20)). Heat is frequently transferred from the bulk substrate to the vessel wall in a jacketed, stirred tank bioreactor. This process can be described by the heat transfer coefficient (α) in Equation (21), which characterizes heat transfer to a wall. Heat conductivity occurs within the vessel wall, which depends on the wall thickness (s) and the material or multiple layers of heat conductivity (λ). Water is mainly a liquid cooling medium that absorbs heat, and heat conductivity occurs in the laminar sublayer region [51].

$$\Delta T_{ar} = \dot{T}_r - T_a \quad (19)$$

$$\Delta T_{aj} = \dot{T}_j - T_a \quad (20)$$

$$q = \frac{\lambda_l}{\delta_{lam}} (T_w - T_\infty) \text{with} : \alpha = \frac{\lambda_l}{\delta_{lam}} \quad (21)$$

Ultimately, these models aim to streamline the complex management of bioreactors by improving their operational efficiency. They focus on regulating reactor temperature and optimizing heat supply to maintain the required thermal conditions, while ensuring an economically viable H_2 production rate and minimising CO_2 emissions [59].

3.2.4. Electrolysis vs. dark-fermentative hydrogen production

Electrolysis powered by renewable electricity remains the leading green method for zero-carbon H_2, yet it supplies under 2 % of global production (Table 1). Its high capital cost is driven by expensive platinum-group catalysts, specialty ion-exchange membranes, and high-pressure electrodes, which can double the LCOH compared to steam methane reforming [60]. The intermittency of solar and wind energy necessitates hybrid systems, which combine photovoltaics, wind farms, energy storage, and backup generation, to maintain continuous operation, further increasing complexity and investment [61]. Beyond generation, a comprehensive green H_2 infrastructure requires multi-megawatt electrolyser facilities, extensive high-pressure pipeline networks, and widespread refuelling stations, necessitating significant cross-sector coordination [62]. Water scarcity compounds these barriers: polymer electrolyte membrane electrolyzers consume 18–25 kg H_2O per kg H_2, while solid oxide electrolyzer cells need 9.1 kg H_2O per kg H_2 [63,64]. Solar field maintenance adds 3.7–5.2 t H_2O per kWp annually for mirror cleaning and cooling [65]. Meeting such volumes often requires desalination, which brings significant energy penalties and generates hypersaline brine that can harm marine and coastal ecosystems. These intertwined challenges, namely CAPEX, intermittency, infrastructure, and water demand, currently limit large-scale deployment and slow the pace of the global H_2 transition [63].

Table 1
Technical and resource comparison of renewable electrolysis versus dark fermentation for hydrogen (H_2) production [62–68].

Criterion	Electrolysis	Dark Fermentation
Market share	<2 %	Emerging
Capital expenditure drivers	Noble-metal catalysts, membranes, and high-pressure cells	Standard fermenters
Water use (H_2O/kg H_2)	Polymer electrolyte membrane: 18–25 kg & Solid oxide electrolyzer cells SOEC: 9.1 kg	Negligible
Intermittency management	Hybrid photovoltaic –wind + storage	Waste-heat integration
Infrastructure intensity	Large electrolyzer farms, pipelines, and stations	Co-location with waste facilities
Operational cost impact	High (water, energy storage)	Low (minimal water, simple heat)

By contrast, DFHP can offer a resource-efficient complement to electrolysis, especially in water- and capital-constrained regions (Table 1). DFHP operates at moderate temperatures without illumination, using mixed microbial consortia to convert organic waste streams into H_2. It eliminates the need for noble-metal catalysts and consumes negligible freshwater, reducing both capital and operational expenses [66]. Although DFHP energy conversion efficiency is lower than that of electrolysis, its minimal water footprint and streamlined infrastructure requirements greatly enhance economic viability [67]. DFHP reactors can be co-located with wastewater treatment plants or agricultural processing facilities, where existing utilities and waste-heat sources maintain optimal fermentation temperatures without grid electricity or extensive pipeline networks [68]. This decentralized, circular model valorises biomass residues and waste heat, promoting local H_2 self-sufficiency and mitigating water stress. Ultimately, while renewable-powered electrolysis is essential for high-purity, large-scale H_2 applications, its substantial capital, water, and infrastructure demands impede rapid scale-up. A diversified H_2 strategy, deploying electrolysis where grid stability, water, and capital are sufficient, and DFHP where they are not, will foster a more resilient, cost-effective transition to a sustainable H_2 economy [69].

3.2.5. Bio-based hydrogen: dual role in waste reduction and energy production

Policy support is needed to enable scalable, cost-effective "bridging technologies" that can drive H_2 production costs to 1 USD/kg by 2030 [4]. Bio-based H_2, derived from organic waste and biomass via gasification, anaerobic digestion, fermentation, and pyrolysis, offers mature, reliable pathways that ensure waste minimization and greenhouse gas emission valorization without competing for grid electricity, making it well-suited for the energy transition across all time horizons [15]. Biomass, often called "green gold," possesses low sulfur content and yields minimal CO_2 during conversion, qualifying it as a clean, renewable feedstock [70]. Two principal routes exist: thermochemical methods (combustion, pyrolysis, gasification) operate at high temperatures (500-2000 °C) and generate H_2-rich syngas and methane streams useable for heat, power, or H_2 production through rapid chemical reactions [71]. Biological processes (anaerobic digestion, dark fermentation, photofermentation, biophotolysis) function at moderate temperatures (25–80 °C) and predominantly produce methane and H_2 as primary products through enzymatic microbial pathways [72]. Thermochemical routes achieve higher processing speeds and H_2 yields per unit time, making gasification economically attractive for large-scale applications with established industrial infrastructure and Technology Readiness Levels (TRL) of 7–9 for commercial deployment. Biological processes offer lower energy requirements, waste valorization capabilities, and carbon-negative potential, though currently limited to pilot-scale demonstrations (TRL 4–6) with commercialization barriers including low yields, long residence times, and limited industrial scalability compared to thermochemical alternatives [73]. The choice of process depends on the feedstock composition and desired outputs, but H_2 or syngas offers greater downstream versatility for net-zero energy systems.

Dark fermentation of biomass currently leads commercial bio-H_2 production, combining long-term maturity with operational simplicity [74]. This technique converts sugar substrates into H_2, CO_2, and organic acids such as acetic, lactic, and butyric acids under strictly anaerobic, light-independent conditions. Reported high conversion efficiencies, and reactors operate effectively across mesophilic (25–40 °C), thermophilic (50–65 °C), compelling thermophilic (65–80 °C), and hyperthermophilic (>80 °C) regimes. Temperature is the chief variable driving microbial metabolism, growth rates, and product profiles. In batch tests, Wang and Wan [75] determined that mixed-culture fermenters attained

peak H_2 yields at 40 °C. Dessì et al. [76] compared activated-sludge dark fermentation across 37 °C, 55 °C, and 70 °C, finding maximum H_2 yields at 55 °C. Jung et al. [77] elucidated that elevated temperatures enhance reaction entropic favorability, accelerate hydrolysis, and broaden microbial diversity, collectively boosting H_2 production in the 50–80 °C range.

A transformative advance involves coupling dark fermentation to industrial waste-heat streams, thereby eliminating the need for external heating fuel and reducing energy losses. Fig. 6 illustrates steam-driven demulsification of liquid petroleum pollutant emulsions: a feed emulsion with 55 % water content was separated at 70 °C using natural gas. The resulting hot-water by-product, currently discarded, can be redirected through the dark fermentation reactor jacket as a free heat source. According to Tang et al. [78], Equation (22) models reactor heat balance. This equation characterizes temperature accumulation in the dark fermentation reactor over time. It considers heat generated from exothermic fermentation reactions and heat release during microbial activity. The model accounts for heat losses through the reactor jacket surrounding the vessel. Additionally, it incorporates heat gains from industrial waste heat recovery systems integrated into the process. This synergy enables self-sustained operation with negligible incremental cost.

$$\frac{[\text{Heat accumulation in the reactor}]}{\text{Unit time}} = \frac{[\text{Heat from reactions}]}{\text{Unit time}} \frac{[\text{Heat exchange}]}{\text{Unit time}} \quad (22)$$

Fig. 7 contrasts two supply chains. Fig. 7a depicts waste-heat integration: industrial hot water circulates through the dark fermentation jacket via a feed pump, providing all required thermal energy for fermentation and eliminating external heating. Fig. 7b shows the renewable electricity chain, i. e, solar, wind, hydro, geothermal, required for electrolytic H_2, highlighting high capital costs, infrastructure complexity, and intermittency management. This juxtaposition underscores how waste-heat utilization slashes both CAPEX and OPEX for green H_2 production.

Techno-economic assessments demonstrate that dark fermentation–photofermentation hybrids credited for waste-heat integration can achieve lower LCOH than standalone electrolysis. Based on experimental pilot-scale demonstrations, Ganguly et al. [79] reported biohydrogen production costs ranging from \$4.0–6.9 kg^{-1} H_2 for cheese whey scenarios at 100 A m^{-2} current density through integrated dark fermentation-microbial electrolysis cell systems. The study utilized validated models incorporating waste-heat recovery from industrial processing facilities. Comparative techno-economic analysis by Romero

Fig. 6. Pictures showing liquid petroleum pollutants emulsions breakdown by steam.

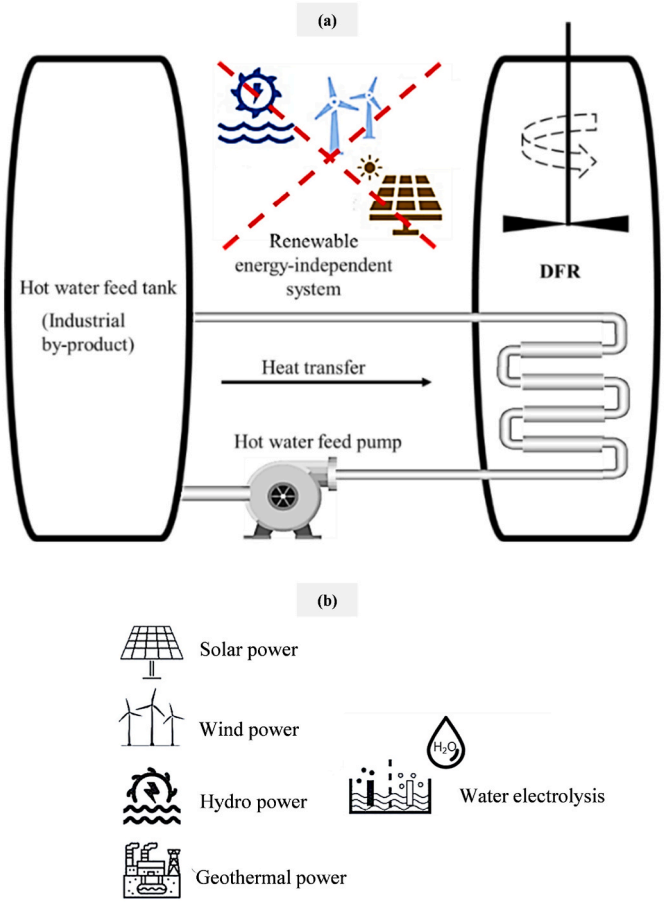

Fig. 7. Process illustration: (a) schematic drawing shows the use of industrial hot water by-products to heat the dark fermentation reactor, reducing waste energy and biohydrogen production cost, and (b) renewable electricity supply chain required for green hydrogen via electrolysis. (For interpretation of the references to colour in this figure legend, the reader is referred to the Web version of this article.)

and Arato [80] demonstrated bio-oil reforming achieved €3.56 kg^{-1} H_2, competitive with natural gas steam reforming at €3.52 kg^{-1} H_2 based on validated economic models for 2700 kg H_2/h facilities. Their analysis incorporated comprehensive capital expenditure (€376 million) and operational expenditure assessments for integrated systems. Waste-heat integration specifically eliminates external heating requirements in dark fermentation reactors operating at optimal temperatures (35–60 °C). The quantified cost reductions result from validated experimental data showing eliminated fuel gas consumption (8754 tonnes/year) and reduced electricity demands through thermal management optimization. These validated assessments confirm commercial viability pathways for integrated biohydrogen production systems utilizing industrial waste streams and thermal energy recovery.

By valorizing existing waste streams and industrial effluents, this approach advances circular economy objectives, reduces environmental footprints, and enables decentralized H_2 production independent of electricity grids [81]. Moreover, dark fermentation's light independence ensures continuous, day-night operation, enhancing reliability. Integrating mature biological processes with readily available waste heat thus represents a resilient, cost-effective pathway to a sustainable H_2 economy, aligning with policy goals to reach 1 USD/kg H_2 by 2030 without waiting for full electrification of energy systems [82].

3.2.6. *Cost evolution of incorporating bio-based hydrogen production and waste-energy recovery*

The global demand for green H_2 is intensifying, with the European Union (EU) targeting the production of up to 10 Mt of H_2 by 2030. This ambition underscores the critical importance of cost competitiveness in H_2 production [83]. A central strategy is the integration of waste-heat recovery to reduce net energy consumption. As dark fermentation capacities scale up, large volumes of excess thermal energy, currently discarded, can instead sustain reactor temperatures, offsetting conventional heating requirements. Economic performance is assessed using the LCOE metric defined by Frassl et al. [84] (Equation (23)):

$$\mathrm{LCOE} = \frac{\sum \frac{\mathrm{CAPEX_t} + \mathrm{OPEX_t} - \mathrm{R_{heat,t}}}{(1+\mathrm{wacc})^t}}{\sum \frac{\mathrm{E_t}}{(1+\mathrm{wacc})^t}} \tag{23}$$

Here, CAPEX denotes capital expenditures, OPEX represents operational expenditures, and wacc is the weighted average cost of capital. In waste-heat-driven dark fermentation systems, recovered thermal energy has zero marginal cost, effectively setting the levelized cost of heat (LCOHeat) to zero and eliminating heat-sales revenues (Rheat = 0). Under these assumptions, the energy transformation efficiency can be estimated using Equation (24):

$$\eta = \frac{E_{out}}{E_{in}} \tag{24}$$

where E_{in} is the energy input, and E_{out} is the reactor's cumulative H_2 energy output.

Because H_2's typical calorific value is 2810 kcal m^{-3} (3.27 kWh m^{-3}), the reactor's E_{out} exceeds its input thermal energy (E_{in}) once η surpasses mid-teens percent. Consequently, modest increases in η yield pronounced LCOH reductions [85]. Frassl et al. [84] demonstrated that leveraging industrial waste heat and improving η significantly enhances economic performance, lowering overall H_2 costs compared to configurations without heat recovery. These results show that valorizing industrial effluent heat not only boosts dark fermentation productivity but also drives H_2 costs down to levels aligned with policy targets. By exploiting free thermal input and maximizing conversion efficiency, dark fermentation systems can deliver green H_2 at competitive prices, advancing the EU's 10 Mt goal without the need for additional renewable electricity infrastructure or fuel procurement [86].

3.2.7. *Life cycle assessment related to dark fermentative hydrogen production (DFHP)*

Life cycle assessment has emerged as a critical evaluation framework for quantifying the environmental sustainability of dark fermentative hydrogen production systems. Recent comprehensive analyses demonstrate that DFHP achieves remarkably low global warming potential compared to conventional hydrogen production pathways [87]. Barghash et al. [88] reported Global Warming Potential (GWP) values of 3.13×10^{-4} kg CO_2-Eq for biohydrogen production with solar energy integration, representing a significant reduction from 4.42×10^{-4} kg CO_2-Eq in conventional processes.

Critical environmental advantages emerge from DFHP's inherent waste valorization capacity. Gören and Özdemir [89] conducted comparative environmental sustainability assessments, revealing that photofermentation achieves the lowest GWP of 1.88 kg-CO_2 eq., while dark fermentation demonstrates substantially lower environmental impacts than thermochemical processes at 4.52 kg-CO_2 eq. However, dark fermentation-microbial electrolysis cell hybrid systems exhibit elevated environmental burdens at 14.6 kg-CO_2 eq./kg H_2 due to substantial electricity requirements.

Energy conversion characteristics represent pivotal sustainability metrics for DFHP systems. Jin et al. [90] demonstrated energy conversion efficiency of 21.43 % from feedstock to product and 62.22 % from hydrolysate to product in wheat straw dark-photo fermentation processes, with total CO_2 emissions of 27.1 kg/h. Water depletion impacts vary significantly, with conventional processes consuming 3.83×10^2 m^3 compared to 2.81×10^{-4} m^3 for biohydrogen production systems.

Carbon-negative biohydrogen production becomes achievable

through integrated dark fermentation approaches. Ganguly et al. [79] quantified GHG emissions of −8.6 and −8.0 kg GHG/kg^{-1} bioH_2 for cheese whey and solid food waste feedstocks, respectively, when coupled with carbon sequestration and renewable electricity resources. These findings demonstrate DFHP's potential for achieving sustainability objectives while contributing to circular economy objectives through integrated waste-to-energy conversion pathways that eliminate fossil fuel dependency and minimize environmental footprints across complete hydrogen production lifecycles [91].

3.3. Emerging challenges and sustainable pathways

DFHP holds immense promise as a low-carbon H_2 pathway. Yet, several interrelated technical and operational challenges hinder its rapid scale-up (Fig. 8). First, the heterogeneity of organic feedstocks, ranging from lignocellulosic agricultural residues to high-nitrogen municipal sludge, leads to wide fluctuations in sugar availability, moisture content, and inhibitory compound levels. These variations cause unstable H_2 yields and unpredictable volatile fatty acid accumulation, complicating reactor control and downstream gas purification [92]. Standardized, low-energy pretreatment approaches, such as mild alkaline hydrolysis or process-heat-driven enzymatic saccharification, can improve substrate uniformity [93]. However, they introduce additional CAPEX and OPEX that must be carefully balanced against gains in productivity. Second, maintaining optimal thermophilic or hyperthermophilic conditions (50–80 °C) is challenging when waste-heat sources are inconsistent or of insufficient temperature quality [94]. In many decentralized settings, such as rural wastewater treatment plants, industrial effluents may only deliver 45–55 °C, below the ideal range for maximal hydrogenase activity. Supplemental electric or biomass heating compensates for these shortfalls but diminishes DFHP's energy advantage. Integrating hybrid solar-thermal collectors or phase-change storage materials within reactor jackets can buffer temperature fluctuations [95]. Nonetheless, incorporating such systems raises design complexity and up-front costs. Third, microbial inhibition by accumulated volatile fatty acids and ammonia presents a persistent barrier. High concentrations of butyrate, acetate, and free ammonia inhibit hydrogenase enzymes and shift metabolic flux toward methanogenesis, reducing H_2 selectivity [96]. Continuous removal of inhibitory metabolites, via in situ membrane pervaporation or adsorption onto low-cost biochars, can sustain microbial performance. Yet, these recovery units add energy demand and maintenance requirements, potentially undermining DFHP's low-energy footprint. Optimizing selective sorbents that regenerate under mild conditions will be critical to retain minimal water and chemical inputs. Fourth, full-scale reactors suffer from mass- and heat-transfer limitations that are negligible at laboratory scale. Large fermenters often develop dead zones where substrate conversion stalls, while local thermal hotspots can denature enzymes. Advanced reactor geometries, such as multi-stage packed-bed or continuous-flow loop designs, promise improved mixing and uniform heat distribution [97]. However, scaling these novel configurations requires extensive pilot-scale demonstrations to validate performance under realistic loading rates and feedstock variability. Finally, valorization of fermentation residues remains underdeveloped. Although volatile fatty acids can be upgraded into bioplastics or platform chemicals, integrating residue streams into existing biorefineries or wastewater infrastructures demands tailored upgrading units and robust logistics [98]. Demonstrating the techno-economic viability of catalytic upgrading, such as volatile fatty acid esterification to produce polyhydroxyalkanoates, in distributed co-location scenarios will be crucial to avoid creating secondary waste and to fully realise circular economy benefits [99].

Overcoming these challenges requires targeted interventions that

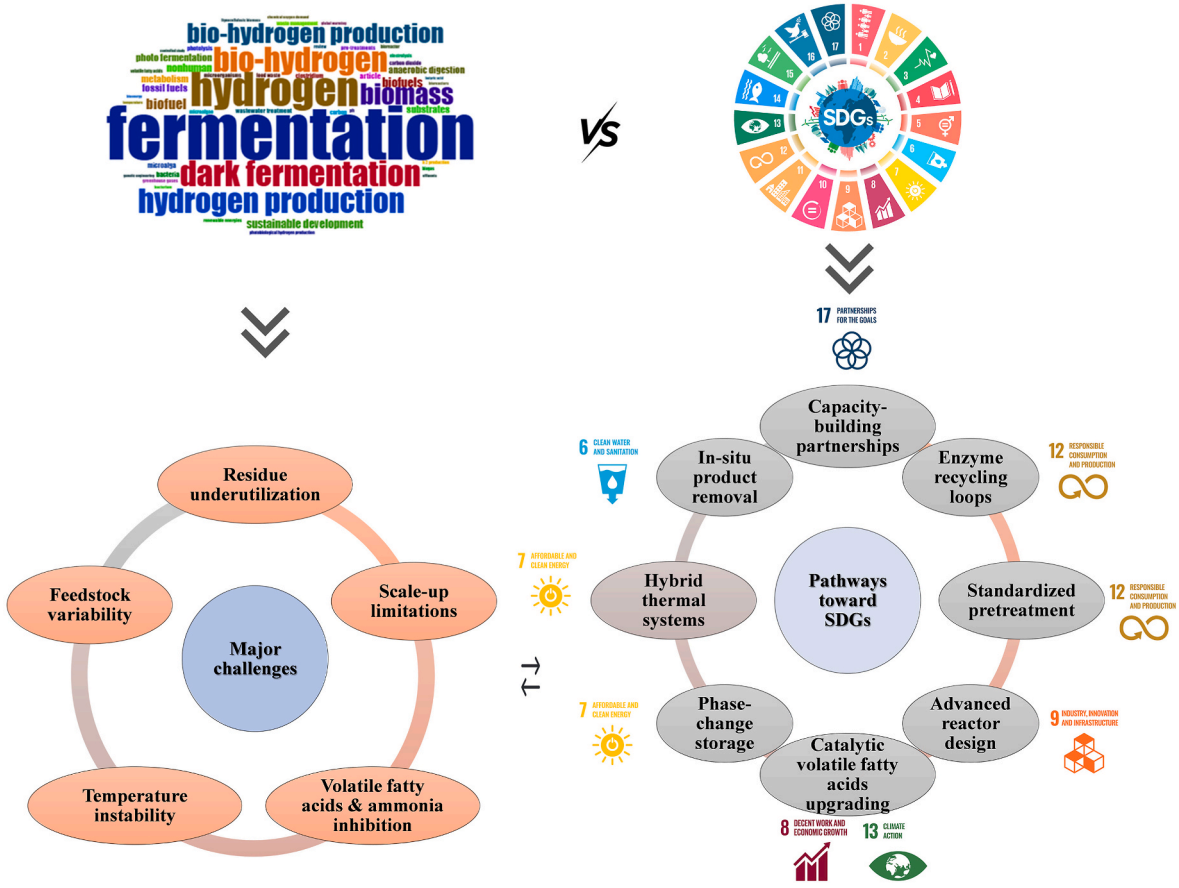

Fig. 8. Dark fermentative biohydrogen production (DFHP) versus sustainable development goals (SDGs): emerging challenges and sustainable pathways.

align with the United Nations SDGs (Fig. 8). To manage feedstock variability (SDG 12: Responsible Consumption and Production), implementing low-energy pretreatments, such as enzyme recycling loops using process heat, can help standardise substrate quality [107]. Pilot studies combining mild alkaline hydrolysis with residual effluent heat recovery should quantify the energy penalties and gains in yield to optimise the cost-benefit trade-offs [100]. Ensuring stable reactor temperatures supports SDG 7: Affordable and Clean Energy. Hybridizing industrial waste-heat streams with solar-thermal collectors or advanced phase-change materials can buffer temperature fluctuations. For instance, coupling 60 °C effluents with parabolic trough collectors feeding a molten-salt storage module can maintain thermophilic conditions during low-effluent-flow periods [101]. Demonstrating modular thermal storage at demonstration sites will inform scalable designs for decentralized applications. Mitigating microbial inhibition advances SDG 6: Clean Water and Sanitation. Embedding in situ product recovery units, such as low-pressure pervaporation membranes or selective adsorption columns, can continuously extract volatile fatty acids and ammonia, preserving hydrogenase activity with minimal water use [102]. Engineering fouling-resistant membranes and low-energy desorption cycles will be vital to sustain DFHP's minimal-water footprint. Addressing scale-up issues aligns with SDG 9: Industry, Innovation and Infrastructure [109]. Establishing pilot-scale facilities that test multi-stage fermenter designs with optimised impellers and baffles will validate mass- and heat-transfer enhancements under realistic throughput conditions [103]. Partnerships between engineering firms and research institutions can standardise modular reactor units that strike a balance between performance gains and simplicity in fabrication and maintenance. Valorizing residues contributes to SDG 13: Climate Action and SDG 8: Decent Work and Economic Growth [108]. Integrating catalytic upgrading units, converting extracted volatile fatty acids into high-value biopolymers or green solvents, creates new revenue streams. Demonstrating such cascaded biorefinery models in agricultural co-operatives can boost local employment, reduce greenhouse-gas emissions from waste disposal, and improve overall process economics [104]. Finally, fostering inclusive partnerships (SDG 17: Partnerships for the Goals) through technology transfer and capacity-building programs is essential. Launching DFHP demonstration sites co-located with municipal wastewater plants or agro-processing facilities in developing regions will generate region-specific performance data, train local operators, and de-risk investment [105]. Such initiatives will catalyse broader adoption of DFHPs, ensure sustainable H_2 access, and accelerate the global energy transition [106].

4. Conclusion and recommendations

A comprehensive bibliometric and techno-economic assessment of DFHP was conducted to map research trends, evaluate process performance, and propose sustainable deployment pathways. Bibliometric analysis was performed on 435 Scopus records, yielding an annual growth rate of 19.61 % and 928 unique keywords. Visualization was conducted using powerful tools, e.g., VOSviewer, Biblioshiny, and Scimago Graphica. For techno-economic evaluation, H_2 conversion efficiencies, water requirements, and cost impacts under waste-heat integration were compared with those of conventional H_2 production methods. DFHP was shown to operate in standard fermenters with negligible water demand. Waste-heat integration was demonstrated to eliminate external heating costs and lower LCOH. Key technical and operational challenges were identified, including feedstock variability, volatile metabolite inhibition, and mass- and heat-transfer limitations at scale. Sustainable pathways were outlined, emphasizing mild alkaline pretreatment, in situ metabolite removal, advanced reactor geometries, and inclusive capacity-building partnerships co-located with waste-processing facilities. The capacity of DFHP to valorize industrial effluents, achieve carbon-neutral operation, and empower resource-limited communities without reliance on scarce catalysts or extensive infrastructure was highlighted. To support large-scale implementation, pilot-scale demonstrations under realistic loading and thermal dynamics are recommended. Detailed life-cycle assessments should be undertaken to quantify cradle-to-grave environmental impacts. Further exploration of process integration with photofermentation and microbial electrolysis is advised to enhance continuous H_2 yields. Finally, the deployment of advanced control strategies utilizing real-time metabolite sensing and machine-learning optimization is encouraged to facilitate commercialization and advance a resilient H_2 economy.

CRediT authorship contribution statement

Moustafa Gamal Snousy: Writing – review & editing, Writing – original draft, Visualization, Validation, Investigation, Conceptualization. **Ashraf R. Abouelmagd:** Supervision, Conceptualization. **Dimitrios E. Alexakis:** Writing – review & editing, Writing – original draft, Visualization, Validation, Resources. **Hassan Mohamed Helmy:** Writing – original draft, Supervision, Investigation, Conceptualization. **Yasser M. Moustafa:** Visualization, Supervision, Conceptualization. **Abdelazim Negm:** Validation. **Erik Weiss:** Validation, Supervision. **Roland Weiss:** Visualization, Supervision. **Esam Ismail:** Writing – review & editing, Supervision, Investigation. **Sayed Mohamed Sakr:** Writing – review & editing, Writing – original draft, Supervision, Investigation. **Abeer El Shahawy:** Writing – review & editing, Writing – original draft, Investigation. **Ahmed M. Saqr:** Writing – review & editing, Writing – original draft, Visualization, Validation, Resources, Investigation, Conceptualization.

Data availability statement

All data presented in the document.

Funding

This research received no external funding.

Declaration of competing interest

The authors declare that they have no known competing financial interests or personal relationships that could have appeared to influence the work reported in this paper.

Acknowledgments

The contribution is a partial output of the project KEGA 032EU-4-2024: Creation of an education model for increasing the skills of students of a non-programming-oriented university in using artificial intelligence tools to support business and entrepreneurship.

References

[1] Syvitski J, Waters CN, Day J, Milliman JD, Summerhayes C, Steffen W, et al. Extraordinary human energy consumption and resultant geological impacts beginning around 1950 CE initiated the proposed anthropocene epoch. Commun Earth Environ 2020;1. https://doi.org/10.1038/s43247-020-00029-y.
[2] Kamsuwan C, Tanprasert S, Nimmanterdwong P, Piemjaiswang R, Saencharee K, Pumchumpol T, et al. Process simulation of cassava cellulosic ethanol production with low to medium-pressure steam heat integration. Energy Rep 2023;9:11–7. https://doi.org/10.1016/j.egyr.2023.04.246.
[3] International Energy Agency (IEA) World Energy Outlook 2022. Paris: IEA Publishing 2022. Available at: https://www.iea.org/reports/world-energy-outlook-2022 (Accessed: 15 October 2025).
[4] Hassan Q, Algburi S, Sameen AZ, Salman HM, Jaszczur M. Green hydrogen: a pathway to a sustainable energy future. Int J Hydrogen Energy 2024;50:310–33. https://doi.org/10.1016/j.ijhydene.2023.08.321.
[5] IEA. Do we need to change our behaviour to reach net zero by 2050? Int Energy Agency Artic 2021;8.
[6] IEA. Global energy review 2021 assessing the effects of economic recoveries on global energy demand and CO2 emissions in 2021. Iea; 2021. p. 10–3.
[7] IEA. Global hydrogen review 2023. Paris: International Energy Agency; 2023.

[8] Bhagwat S, Olczak M. Green hydrogen : bridging the energy transition in Africa and Europe, vol. 33. FSR Glob; 2020.
[9] UN General Assembly. Transforming our world: the 2030 Agenda for Sustainable Development, A/RES/70/1, 2015. Available at: https://sdgs.un.org/2030agenda (Accessed: 15 October 2025).
[10] Snousy MG, Abouelmagd AR, Moustafa YM, Gamvroula DE, Alexakis DE, Ismail E. The potential role of Africa in green hydrogen production: a short-term roadmap to protect the world's future from climate crisis. Water (Switzerland) 2025;17. https://doi.org/10.3390/w17030416.
[11] Hosseini SE, AbdulWahid M. Hydrogen production from renewable and sustainable energy resources: promising green energy carrier for clean development. Renew Sustain Energy Rev 2016;57:850–66.
[12] Marchetti C. On hydrogen and energy systems. Int J Hydrogen Energy 1976;1: 3–10. https://doi.org/10.1016/0360-3199(76)90004-5.
[13] Hosseini SE. Transition away from fossil fuels toward renewables: lessons from Russia-Ukraine crisis. Futur Energy 2022;1:2–5. https://doi.org/10.55670/fpll.fuen.1.1.8.
[14] Liadze I, Macchiarelli C. The economic costs of the Russia-Ukraine conflict. Natl Inst Econ Soc Res NIESR Policy 2022;32:1–5.
[15] Zainal BS, Ker PJ, Mohamed H, Ong HC, Fattah IMR, Rahman SMA, et al. Recent advancement and assessment of green hydrogen production technologies. Renew Sustain Energy Rev 2024;189. https://doi.org/10.1016/j.rser.2023.113941.
[16] IRENA. Global hydrogen trade to meet the 1.5°C climate goal: part I - trade outlook for 2050 and way forward. Glob Hydrog Trade to Meet 15°C Clim Goal Trade Outlook 2050 W Forw 2022;114.
[17] Belward A, Bisselink B, Bódis K. Renewable energies in africa–current knowledge. In: Belward A, Bisselink B, Bódis K, Al, editors. Renew energies Africa–current knowledge monforti-ferrario, F. 633 EUR 25108 EN Luxemb (Luxembourg) Publ Off Eur Union, JRC67752 2011; 2011.
[18] Rolo I, Costa VAF, Brito FP. Hydrogen-based energy systems: current technology development status, opportunities and challenges. Energies 2024;17. https://doi.org/10.3390/en17010180.
[19] Tavakoli M, Motlagh ZK, Dąbrowska D, Youssef YM, Đurin B, Saqr AM. Harnessing AHP and fuzzy scenarios for resilient flood management in arid environments: challenges and pathways toward sustainability. Water 2025;17: 1276. https://doi.org/10.3390/w17091276.
[20] Jayachandran V, Basak N, De Philippis R, Adessi A. Novel strategies towards efficient molecular biohydrogen production by dark fermentative mechanism: present progress and future perspective. Bioproc Biosyst Eng 2022;45:1595–624. https://doi.org/10.1007/s00449-022-02738-4.
[21] Krupp M, Widmann R. Biohydrogen production by dark fermentation: experiences of continuous operation in large lab scale. Int J Hydrogen Energy 2009;34:4509–16. https://doi.org/10.1016/j.ijhydene.2008.10.043.
[22] Ranade VV, Chaudhari RV, Gunjal PR. Trickle bed reactors: reactor engineering and applications. Trickle Bed React React Eng Appl 2011:1–274. https://doi.org/10.1016/C2009-0-16553-4.
[23] Periyasamy S, Gopalakrishnan K, Péter B, Sang-Hyoun K, Takurou K, Qin XK, et al. A critical review on issues and overcoming strategies for the enhancement of dark fermentative hydrogen production in continuous systems. Int J Hydrogen Energy 2016;41:3820–36.
[24] Jain R, Panwar NL, Jain SK, Gupta T, Agarwal C, Meena SS. Bio-hydrogen production through dark fermentation: an overview. Biomass Convers Biorefinery 2024;14:12699–724. https://doi.org/10.1007/s13399-022-03282-7.
[25] Saqr AM, Pant RR, Alao JO, Chaurasia PK, Abdelkebir B, Abd-Elmaboud ME. Soil remediation through washing and flushing: bibliometric trends, technical review, and future prospects. Environ Earth Sci 2025;84:401. https://doi.org/10.1007/s12665-025-12386-y.
[26] Aria M, Cuccurullo C. Bibliometrix: an R-tool for comprehensive science mapping analysis. J Informetr 2017;11:959–75. https://doi.org/10.1016/j.joi.2017.08.007.
[27] Van Eck NJ, Waltman L. VOS: a new method for visualizing similarities between objects. Stud Classif Data Anal Knowl Organ 2007:299–306. https://doi.org/10.1007/978-3-540-70981-7_34.
[28] Hassan-Montero Y, De-Moya-anegón F, Guerrero-Bote VP. SCImago graphica: a new tool for exploring and visually communicating data. Prof La Inf 2022;31. https://doi.org/10.3145/epi.2022.sep.02.
[29] Saqr AM, Nasr M, Fujii M, Yoshimura C, Ibrahim MG. Integrating MODFLOW-USG and Walrus Optimizer for Estimating Sustainable Groundwater Pumping in Arid Regions Subjected to Severe Drawdown. Springer Water Part 2025:127–43. https://doi.org/10.1007/978-3-031-79122-2_5. F9.
[30] Timilsina B, Kharel M, Shrestha R, Saqr AM, Pant RR. Assessment of soil quality along the elevation gradient of the Seti River watershed in Pokhara Metropolitan City, Nepal. Environ Monit Assess 2025;197. https://doi.org/10.1007/s10661-025-13716-0.
[31] Pisani N, Boekhout HD, Heemskerk EM, Take FW. China's rise as global scientific powerhouse: a trajectory of international collaboration and specialization in high-impact research. SSRN Electron J; 2024. https://doi.org/10.2139/ssrn.5014244.
[32] Yuan R, Pu J, Wu D, Wu Q, Huhe T, Lei T, et al. Research priorities and trends on bioenergy: insights from bibliometric analysis. Int J Environ Res Publ Health 2022;19. https://doi.org/10.3390/ijerph192315881.
[33] Slater SC, Simmons BA, Rogers TS, Phillips MF, Nordahl K, Davison BH. The DOE bioenergy research centers: history, operations, and scientific output. Bioenergy Res 2015;8:881–96. https://doi.org/10.1007/s12155-015-9660-8.
[34] Du YH, Wang MY, Yang LH, Tong LL, Guo DS, Ji XJ. Optimization and Scale-Up of fermentation processes driven by models. Bioengineering 2022;9. https://doi.org/10.3390/bioengineering9090473.
[35] Amusa AA, Johari A, Yahaya SA. Advancing biomass pyrolysis: a bibliometric analysis of global research trends (2002–2022). Environ Dev Sustain 2025;27: 8265–316. https://doi.org/10.1007/s10668-023-04292-9.
[36] Incer-Valverde J, Korayem A, Tsatsaronis G, Morosuk T. "Colors" of hydrogen: definitions and carbon intensity. Energy Convers Manag 2023;291. https://doi.org/10.1016/j.enconman.2023.117294.
[37] Neacsa A, Eparu CN, Stoica DB. Hydrogen–natural gas blending in distribution systems—an energy, economic, and environmental assessment. Energies 2022;15. https://doi.org/10.3390/en15176143.
[38] IRENA. REmap 2030 - a renewable energy roadmap. Publications/2014/Jun/REmap-2030-Full-Report 2014:188.
[39] Sołowski G, Konkol I, Cenian A. Methane and hydrogen production from cotton waste by dark fermentation under anaerobic and micro-aerobic conditions. Biomass Bioenergy 2020;138. https://doi.org/10.1016/j.biombioe.2020.105576.
[40] Jensterle M, Narita J, Piria R, Samadi S, Prantner M, Crone K, et al. The role of clean hydrogen in the future energy systems of Japan and Germany. Adelphi 2019;6:130.
[41] Ayodele TR, Munda JL. The potential role of green hydrogen production in the South Africa energy mix. J Renew Sustain Energy 2019;11. https://doi.org/10.1063/1.5089958.
[42] El-Araby R. Biofuel production: exploring renewable energy solutions for a greener future. Biotechnol Biofuels Bioprod 2024;17. https://doi.org/10.1186/s13068-024-02571-9.
[43] Pretoria MP. Green hydrogen: a potential export commodity in a new global marketplace. TipsOrgZaM PatelTrade Ind Policy Strateg Pretoria, South Africa, 2020•tipsOrgZa; 2020.
[44] Acar C, Dincer I. Review and evaluation of hydrogen production options for better environment. J Clean Prod 2019;218:835–49. https://doi.org/10.1016/j.jclepro.2019.02.046.
[45] Sarker AK, Azad AK, Rasul MG, Doppalapudi AT. Prospect of green hydrogen generation from hybrid renewable energy sources: a review. Energies 2023;16. https://doi.org/10.3390/en16031556.
[46] Hallenbeck PC. Fundamentals of the fermentative production of hydrogen. Water Sci Technol 2005;52:21–9. https://doi.org/10.2166/wst.2005.0494.
[47] Hu M, Xuan F, Shao H. A novel measurement method of temperature model for bioreactor. Front Electr Electron Eng China 2010;5:218–23. https://doi.org/10.1007/s11460-010-0002-5.
[48] Pachauri N, Singh V, Rani A. Two degree of freedom PID based inferential control of continuous bioreactor for ethanol production. ISA Trans 2017;68:235–50. https://doi.org/10.1016/j.isatra.2017.03.014.
[49] Okonkwo O, Escudie R, Bernet N, Mangayil R, Lakaniemi AM, Trably E. Bioaugmentation enhances dark fermentative hydrogen production in cultures exposed to short-term temperature fluctuations. Appl Microbiol Biotechnol 2020; 104:439–49. https://doi.org/10.1007/s00253-019-10203-8.
[50] Zhang Q, Jiao Y, He C, Ruan R, Hu J, Ren J, et al. Biological fermentation pilot-scale systems and evaluation for commercial viability towards sustainable biohydrogen production. Nat Commun 2024;15. https://doi.org/10.1038/s41467-024-48790-4.
[51] Müller M, Husemann U, Greller G, Meusel W, Kraume M. Heat transfer characteristics of a stirred single-use bioreactor. Biochem Eng J 2018;140: 168–77. https://doi.org/10.1016/j.bej.2018.09.022.
[52] Bergamo CM, Di Monaco R, Ratusznei SM, Rodrigues JAD, Zaiat M, Foresti E. Effects of temperature at different organic loading levels on the performance of a fluidized-bed anaerobic sequencing batch bioreactor. Chem Eng Process Process Intensif 2009;48:789–96. https://doi.org/10.1016/j.cep.2008.10.003.
[53] Zhou Z, Song B, Zhu L, Li Z, Wang Y. Optimizing of bioreactor heat supply and material feeding by numerical calculation. Commun Comput Inf Sci 2011;135: 195–202. https://doi.org/10.1007/978-3-642-18134-4_31.
[54] Tang X, Xu B. Reactor temperature compound control strategy based on disturbance observer. IEEE Access 2023;11:84554–64. https://doi.org/10.1109/ACCESS.2023.3303036.
[55] Li ZN, Chu MS, Liu ZG, Ruan GJ, Li BF. Furnace heat prediction and control model and its application to large blast furnace. High Temp Mater Process 2019;38: 884–91. https://doi.org/10.1515/htmp-2019-0049.
[56] Zhan J, Du J, Dong S, Hu W. Superheated steam temperature system of thermal power control engineering based on neural network local multi-model prediction. Therm Sci 2021;25:2949–56. https://doi.org/10.2298/TSCI2104949Z.
[57] Wang H, Kehoe D, Murrell J, Jing D. Structured methodology for process development in scalable stirred tank bioreactors platforms. Bioprocess Cell Based Ther 2016:35–64. https://doi.org/10.1002/9781118743362.ch2.
[58] Tusset AM, Inacio D, Fuziki MEK, Costa PMLZ, Lenzi GG. Dynamic analysis and control for a bioreactor in fractional order. Symmetry 2022;14. https://doi.org/10.3390/sym14081609.
[59] Mansilla C, Sigurvinsson J, Bontemps A, Maréchal A, Werkoff F. Heat management for hydrogen production by high temperature steam electrolysis. ECOS 2005 - proc 18th int conf effic cost. Optim Simulation, Environ Impact Energy Syst; 2005. p. 1159–66.
[60] Nicita A, Maggio G, Andaloro APF, Squadrito G. Green hydrogen as feedstock: financial analysis of a photovoltaic-powered electrolysis plant. Int J Hydrogen Energy 2020;45:11395–408. https://doi.org/10.1016/j.ijhydene.2020.02.062.
[61] Elminshawy NAS, Diab S, Yassen YES, Elbaksawi O. An energy-economic analysis of a hybrid PV/wind/battery energy-driven hydrogen generation system in rural regions of Egypt. J Energy Storage 2024;80. https://doi.org/10.1016/j.est.2023.110256.

[62] Snousy MG, Helmy HM, Wu J, Zawrah MF, Abouelmagd A. Nanotechnology for water treatment: is it the best solution now? J Earth Sci 2023;34:1616–20. https://doi.org/10.1007/s12583-023-1928-8.
[63] Barghash H, Al Farsi A, Okedu KE, Al-Wahaibi BM. Cost benefit analysis for green hydrogen production from treated effluent: the case study of Oman. Front Bioeng Biotechnol 2022;10. https://doi.org/10.3389/fbioe.2022.1046556.
[64] Wang Y, Wen C, Tu J, Zhan Z, Zhang B, Liu Q, et al. The multi-scenario projection of cost reduction in hydrogen production by proton exchange membrane (PEM) water electrolysis in the near future (2020–2060) of China. Fuel 2023;354. https://doi.org/10.1016/j.fuel.2023.129409.
[65] Yang D, Liu J, Yang J, Ding N. Life-cycle assessment of China's multi-crystalline silicon photovoltaic modules considering international trade. J Clean Prod 2015; 94:35–45. https://doi.org/10.1016/j.jclepro.2015.02.003.
[66] Su H, Cheng J, Zhou J, Song W, Cen K. Combination of dark- and photo-fermentation to enhance hydrogen production and energy conversion efficiency. Int J Hydrogen Energy 2009;34:8846–53. https://doi.org/10.1016/j.ijhydene.2009.09.001.
[67] Hussien M, Mohamed HO, Jadhav DA, Bahaa A, Jo SM, Jang JH, et al. Synergistic integration of dark fermentation and microbial electrolysis cells for hydrogen production and sustainable swine manure treatment. Int J Hydrogen Energy 2025;115:299–309. https://doi.org/10.1016/j.ijhydene.2025.02.453.
[68] Montiel-Corona V, Buitrón G. Practical applications of dark fermentation for hydrogen production. Springer Water 2024;F3093:47–66. https://doi.org/10.1007/978-3-031-57735-2_4. Part.
[69] Hosseini SE. Hydrogen diplomacy. Hydrog Dipl 2024. https://doi.org/10.55670/fpll.book/1.
[70] Zamri MFMA, Hasmady S, Akhiar A, Ideris F, Shamsuddin AH, Mofijur M, et al. A comprehensive review on anaerobic digestion of organic fraction of municipal solid waste. Renew Sustain Energy Rev 2021;137. https://doi.org/10.1016/j.rser.2020.110637.
[71] Osman IA, Mehta N, Elgarahy MA, et al. Conversion of biomass to biofuels and life cycle assessment: a review. Environ Chem Lett 2021;19:4075–118.
[72] Ingaldi M, Klimecka-Tatar D. People's attitude to energy from hydrogen—from the point of view of modern energy technologies and social responsibility. Energies 2020;13. https://doi.org/10.3390/en13246495.
[73] Pranay Rajendra Lanjekar, Narayan Lal Panwar. A review on hydrogen production from biomass and commercialization assessment through technology readiness levels (TRLs). Bioenergy Res 2023;17:912–31.
[74] Liu S, Zhu J, Chen M, Xin W, Yang Z, Kong L. Hydrogen production via catalytic pyrolysis of biomass in a two-stage fixed bed reactor system. Int J Hydrogen Energy 2014;39:13128–35. https://doi.org/10.1016/j.ijhydene.2014.06.158.
[75] Wang J, Wan W. Effect of temperature on fermentative hydrogen production by mixed cultures. Int J Hydrogen Energy 2008;33:5392–7. https://doi.org/10.1016/j.ijhydene.2008.07.010.
[76] Dessì P, Lakaniemi AM, Lens PNL. Biohydrogen production from xylose by fresh and digested activated sludge at 37, 55 and 70 °C. Water Res 2017;115:120–9. https://doi.org/10.1016/j.watres.2017.02.063.
[77] Jung KW, Kim DH, Kim SH, Shin HS. Bioreactor design for continuous dark fermentative hydrogen production. Bioresour Technol 2011;102:8612–20. https://doi.org/10.1016/j.biortech.2011.03.056.
[78] Tang X, Xu B, Xu Z. Reactor temperature control based on improved fractional order self-anti-disturbance. Processes 2023;11. https://doi.org/10.3390/pr11041125.
[79] Ganguly A, Sun P, Liu X, Delgado HE, Sun L, Elgowainy A. Techno-economic and life cycle analysis of bio-hydrogen production using bio-based waste streams through the integration of dark fermentation and microbial electrolysis. Green Chem 2025;27:6213–31. https://doi.org/10.1039/d4gc05020g.
[80] Romero MJA, Arato E. Assessment of the techno-economic viability to produce biohydrogen from biowaste. Chem Eng Trans 2025;117:541–6. https://doi.org/10.3303/CET25117091.
[81] Toklu E, Coskun Avci A, Kaygusuz K, Gur M. A research on hydrogen production from industrial waste heat by thermal water splitting. Int J Hydrogen Energy 2016;41:10071–9. https://doi.org/10.1016/j.ijhydene.2015.12.131.
[82] Jimena M, Luna L. Hydrogen as a potential renewable and secure source for energy supply. Environ Technol Int Aff Hydrog 2019:1–74.
[83] Böhm H, Moser S, Puschnigg S, Zauner A. Power-to-hydrogen & district heating: technology-based and infrastructure-oriented analysis of (future) sector coupling potentials. Int J Hydrogen Energy 2021;46:31938–51. https://doi.org/10.1016/j.ijhydene.2021.06.233.
[84] Frassl N, Sistani NR, Wimmer Y, Kapeller J, Maggauer K, Kathan J. Techno-economic assessment of waste heat recovery for green hydrogen production: a simulation study. Elektrotechnik Und Informationstechnik 2024;141:288–98. https://doi.org/10.1007/s00502-024-01231-y.
[85] Jiang J, Hu J, Cui M, Tian H. Integration of hydrogen production and waste heat recovery in electrochemical wastewater treatment. Renew Energy 2012;43: 179–82. https://doi.org/10.1016/j.renene.2011.12.007.
[86] Giakoumakis G, Sidiras D. Production and storage of hydrogen from biomass and other sources: technologies and policies. Energies 2025;18. https://doi.org/10.3390/en18030650.
[87] Wu D, Gao Z, Wu S, Xiao R. Negative net global warming potential hydrogen production through biomass gasification combined with chemical looping: environmental and economic assessments. Int J Hydrogen Energy 2024;66:24–32. https://doi.org/10.1016/j.ijhydene.2024.04.078.
[88] Barghash H, AlRashdi Z, Okedu KE, Desmond P. Life-cycle assessment study for bio-hydrogen gas production from sewage treatment plants using solar PVs. Energies 2022;15. https://doi.org/10.3390/en15218056.
[89] Goren AY, Dincer I, Khalvati A. Comparative environmental sustainability assessment of biohydrogen production methods. Sci Total Environ 2023;904. https://doi.org/10.1016/j.scitotenv.2023.166613.
[90] Jin M, Wei X, Mu X, Ren W, Zhang S, Tang C, et al. Life-cycle analysis of biohydrogen production via dark-photo fermentation from wheat straw. Bioresour Technol 2024;396. https://doi.org/10.1016/j.biortech.2024.130429.
[91] Derwent RG. Intercomparison of the mechanisms of hydrogen generation from the oxidation of organic compounds: consequences for the global warming potential (GWP) for hydrogen. Int J Hydrogen Energy 2025;148. https://doi.org/10.1016/j.ijhydene.2025.150116.
[92] Wainaina S, Lukitawesa Kumar Awasthi M, Taherzadeh MJ. Bioengineering of anaerobic digestion for volatile fatty acids, hydrogen or methane production: a critical review. Bioengineered 2019;10:437–58. https://doi.org/10.1080/21655979.2019.1673937.
[93] Koradiya M. Advances in enzymatic hydrolysis and saccharification technology. Biofuels Sci Explor Technol a Sustain Environ 2024:83–114. https://doi.org/10.1201/9781003350606-7.
[94] Rodríguez-Jiménez LM, Pérez-Vidal A, Torres-Lozada P. Research trends and strategies for the improvement of anaerobic digestion of food waste in psychrophilic temperatures conditions. Heliyon 2022;8:e11174. https://doi.org/10.1016/j.heliyon.2022.e11174.
[95] Liu B, Zhang X, Ji J. Review on solar collector systems integrated with phase-change material thermal storage technology and their residential applications. Int J Energy Res 2021;45:8347–69. https://doi.org/10.1002/er.6397.
[96] Campbell A, Gdanetz K, Schmidt AW, Schmidt TM. H2 generated by fermentation in the human gut microbiome influences metabolism and competitive fitness of gut butyrate producers. Microbiome 2023;11. https://doi.org/10.1186/s40168-023-01565-3.
[97] Baharudin L, Indera LAA, Watson MJ, Yip ACK. Process intensification in multifunctional reactors: a review of multi-functionality by catalytic structures, internals, operating modes, and unit integrations. Chem Eng Process Process Intensif 2021;168. https://doi.org/10.1016/j.cep.2021.108561.
[98] Koubaa M. Integrated biorefinery for a next-generation methanization process focusing on volatile fatty acid valorization: a critical review. Molecules 2024;29. https://doi.org/10.3390/molecules29112477.
[99] Amabile C, Abate T, Muñoz R, Chianese S, Musmarra D. Techno-economic assessment of biopolymer production from methane and volatile fatty acids: effect of the reactor size and biomass concentration on the poly(3-hydroxybutyrate-co-3-hydroxyvalerate) selling price. Sci Total Environ 2024;929. https://doi.org/10.1016/j.scitotenv.2024.172599.
[100] Mkilima T. Hydrothermal liquefaction of wastewater as part of tailoring biocrude composition for a circular bioeconomy: a review. Biofuel Bioprod Biorefining 2025. https://doi.org/10.1002/bbb.70004.
[101] Sahu P. A comprehensive review of saline effluent disposal and treatment: conventional practices, emerging technologies, and future potential. J Water Reuse Desalin 2021;11:33–65. https://doi.org/10.2166/wrd.2020.065.
[102] Santos AG, de Albuquerque TL, Ribeiro BD, Coelho MAZ. In situ product recovery techniques aiming to obtain biotechnological products: a glance to current knowledge. Biotechnol Appl Biochem 2021;68:1044–57. https://doi.org/10.1002/bab.2024.
[103] Moresi M. Design and operation of a multifunctional pilot-scale bioreactor for enhanced aerobic fermentation. Fermentation 2025;11. https://doi.org/10.3390/fermentation11020101.
[104] Barros MV, de Jesus RHG, Ribeiro BS, Piekarski CM. Going in circles: key aspects for circular economy contributions to agro-industrial cooperatives. Circ Econ Sustain 2023;3:861–80. https://doi.org/10.1007/s43615-022-00211-8.
[105] Alley KD. Microbial machines: experiments with decentralized wastewater treatment and reuse in India. Microb Mach Exp with Decentralized Wastewater Treat Reuse India 2023:1–210.
[106] Saqr AM, Abd-Elmaboud ME. Management of Saltwater Intrusion in Coastal Aquifers: A Review and Case Studies from Egypt. Online J. Eng. Sci. 2024;3:1–17. https://doi.org/10.31586/ojes.2024.982.
[107] Snousy MG, Elshafie HM, Abouelmagd AR, Hassan NE, Abd-Elmaboud ME, Mohammadi AA, Elewa AMT, EL-Sayed E, Saqr AM. Enhancing the prediction of groundwater quality index in semi-arid regions using a novel ANN-based hybrid arctic puffin-hippopotamus optimization model. J. Hydrol. Reg. Stud. 2025;59. https://doi.org/10.1016/j.ejrh.2025.102424.
[108] Saqr AM, Kartal V, Karakoyun E, Abd-Elmaboud ME. Improving the Accuracy of Groundwater Level Forecasting by Coupling Ensemble Machine Learning Model and Coronavirus Herd Immunity Optimizer. Water Resour. Manag. 2025 https://doi.org/10.1007/s11269-025-04210-w.
[109] Alao JO, Saqr AM, Ayejoto DA, Otorkpa OJ, Abubakar F, Mohammed MAA, Ibe AA. Environmental Impacts of Hydrocarbon Contaminants and Associated Potential Public Health Risks. J. Hazard. Mater. Adv. 2025;19:100853. https://doi.org/10.1016/j.hazadv.2025.100853.